## 39.0 SOLUTE AND PRECIPIATE EFFECTS ON MAGNESIUM RECRYSTALLIZATION

Gillian Storey (Mines)
Faculty: Amy Clarke and Kester Clarke (Mines)
Industrial Mentors: Scott Sutton and Dan Hartman (Mag Specialties Inc.)

This project was initiated in Fall 2019. The research performed during this project will serve as the basis for a Master's thesis program for Gillian Storey.

### 39.1 Project Overview and Industrial Relevance

This project is a comparative study on the effects of varying precipitate and solute content on recrystallization kinetics in Mg alloys. According to ASTM B91-17 standard, ZK60-based alloys have compositions that are nominally Mg-5.8 Zn-0.65 Zr (wt.%) with some other possible additions [39.1]. These alloys are ideally suited for this study because they are commercial alloys with insoluble zirconium particles that influence grain size and recrystallization [39.2]. ZK60 is a typical extrusion alloy that experiences age (precipitation) hardening [39.3]. During wrought processing followed by extrusion, recrystallization initiates at grain boundaries. Relative to alloys such as Mg-6.2 Zn (Z6), ZK60 exhibits a finer microstructure after solidification, hot work, or annealing processes due to Mg(Zn) precipitates that inhibit grain growth [39.2]. The determination of classical Avrami parameters and Zener pinning parameters for static recrystallization will be adapted to dynamic recrystallization and hot working. This will determine the effect of microstructural development kinetics on hot working parameters and material properties.

Microstructural characterization and texture evaluation through electron backscatter diffraction (EBSD) is essential to develop a kinetics model based on percent recrystallization at each time and temperature of heat treatment. An anticipated experimental outcome is that there should be a significant effect of precipitates on recrystallization behavior due to Zener pinning, yet only a minor effect from Zn solute content. Uniaxial compression tests at common extrusion temperatures (300 °C/573K, 350 °C/623K, 400 °C/673K), using a Gleeble® 3500 thermomechanical simulator, allows for the simulation of different dynamic recrystallization (DRX) conditions. The occurrence of DRX can be identified from the presence of stress peaks in flow curves, and in some situations, inflection points of $\ln\varepsilon$-$\ln\sigma$ [39.4]. These observations can then be confirmed through microstructural characterization. Understanding the initiation of dynamic recrystallization for constant strain rate hot deformation processes further helps to define optimal industrial processing parameters for ZK60.

### 39.2 Previous Work

ZK60 does not have a standard composition beyond the nominal Mg-5.8 Zn-0.65 Zr (wt.%), and various rare earth elements can be added. Rare earth elements, such as cerium and lanthanum, can be added to improve high temperature strength and creep resistance [39.4]. Although the specific compositions of ZK60 being examined for this research program have not been previously evaluated, there are publications on the effects of alloying, temperature, extrusion parameters on ZK60 with various other compositions [39.8, 38.11].

The driving force for recrystallization in magnesium alloys is either thermal or strain energys [39.5].The progressive lattice rotation at grain boundaries provides a location for recrystallization to occur. Local shearing near grain boundaries, as shown in **Figure 39.1**, occurs during lower temperature deformation of magnesium alloys via basal slip due to a lack of five independent slip systems required for homogenous plasticity. Dynamic recovery of dislocations results in new grains/subgrains. This process is progressive, with no clear division between nucleation and growth stages. At higher deformation temperatures, non-basal slip is activated and deformation is more homogenous [39.5].

Research into microstructural changes of ZK60 throughout the DRX process lends an improved understanding of the process on the phenomenological level, however industry is lacking an understanding of the underlying processing parameters that control DRX. During hot deformation of materials with low to moderate stacking fault energy (SFE) at medium (500K-523K) and high temperatures (>523K), the formation of new grains occurs by conventional DRX—i.e., twinning [39.6], nucleation by bulging of dislocation tangles [39.7], and subgrain rotation [39.7].

Recently, recently observed mechanisms of DRX have been found to operate at lower temperatures (473-500K), including basal slip and mechanical twinning. 39.8]. DRX mechanisms are directly related to deformation conditions and therefore are affected by operating parameters of deformation processes, including strain rate and temperature. Despite this information, not enough quantitative data is available in the literature to elucidate an interdependence of deformation and specific DRX mechanisms in ZK60 magnesium alloys.

The standards for extrusion of magnesium alloys in industry include ASTM B107/B107M-13 [37.9]. This standard is the general guideline for magnesium-alloy extrusion of bars, rods, profiles, tubes, and wires. There is no specific standard for ZK60, yet in industry the B107/B107M-13 standard is adjusted to better suit the mechanical properties of ZK60. The minimum requirements for tensile strength, yield strength, and elongation for ZK60 outlined in this standard differ depending on the geometry and cross section of the extrudate. For bars, rods, and wire forms of ZK60 the minimum tensile strength and yield strength are respectively 43.0 and 31.0 ksi [37.9]. Additionally, there are dimensional tolerances included in this standard for straightness, length, angles, roughness, radius, and flatness. The experimental ZK60 material used for this project conforms to B107/B107M-13 standards.

The flow curves for a ZK60 alloy with the specific composition of Mg-5.8% Zn-0.65%Zr (wt%), processed through chill casting and homogenization heat treatment at varying deformation temperatures, are included in **Figure 39.2**. It is characteristic for flow stress to increase to a maximum, and then decrease to a steady state under circumstances of hot working accompanied by DRX [39.8]. At low temperatures, the flow curve exhibits high peak stress then negligible work softening after the peak. At moderate temperatures, both peak stress and peak strain are high, but work softening is very pronounced after the peak. At the highest temperatures, steady state is attained after small peak stress and strain, with very minimal work softening. These correlations allow further evaluation of peak stress and activation parameters, as well as activation energy required for DRX.

Metallography after compression testing at a variety of temperatures and strain rates can lend insight into active deformation mechanisms. These observations revealed features of nucleation of DRX during plastic deformation at moderate and high temperatures. At lower temperatures (473-500K), ZK60 samples exhibited twinning and dislocation glide [39.8]. These lower temperatures also revealed progressive lattice rotations in areas of high dislocation density near twin boundaries, resulting in formation of finer grains with non-equilibrium grain boundaries. Basal slip is dominant, yet there are also short thin slip lines at an acute angle to the basal slip lines. Micrographs of deformation structure from deformation at various temperatures are included as **Figure 39.3** [39.8]. For ZK60 (Mg-5.8% Zn-0.65% Zr (wt%)), lower temperatures (473-500K) exhibited basal slip and mechanical twinning to accommodate plastic deformation. Moderate temperature (500-523K) deformation is associated with cross-slip-assisted dislocation glide. At higher temperatures (>523K), deformation is diffusion controlled and accompanied by dislocation climb [39.8].

## 39.3 Recent Progress

### 39.3.1 Sample Preparation

Optimization of sectioning, mounting, and polishing is a necessary step required to perform high quality metallography on the experimental materials. ZK60, like all magnesium alloys, is relatively soft and introducing deformation regions is especially easy and must be carefully avoided to observe the as-processed microstructure. These deformation regions can skew results and impede analysis through electron backscatter diffraction (EBSD). Test samples of an initial trial ZK60 alloy were sectioned with a high-speed abrasive wheel, ground with 600 grit grinding paper, then mounted in cold epoxy. This cold epoxy has a maximum curing temperature of 40°C and is allowed to cure for 24 hours. These samples were then further ground to 1200 grit and then polished sequentially using 6$\mu$m, 3$\mu$m, and 1 $\mu$m diamond suspension. The specimens were cleaned between every polishing step by rinsing with water, washing with a soapy cotton ball, rinsing in water again, removing water with ethanol, and then hot air blow drying. Optical microscopy was performed between every diamond abrasive step to ensure adequate polishing. These samples were then vibropolished in a water-free 0.5 $\mu$m colloidal silica solution for 2 hours. After doing this colloidal silica polishing step there were visible pits caused on the surface of each sample. In the future instead of vibropolishing, samples will be polished using the water-free 0.5 $\mu$m colloidal silica solution on a neoprene polishing pad for 3 minutes using moderate force. The etchant used on samples that were only polished to 1 $\mu$m diamond suspension was a solution of 3g picric acid, 10mL acetic acid, 70mL ethanol, and 10mL of distilled

water for approximately 15-20 seconds. This etchant was very effective for grain definition. Optical micrographs of trial ZK60 material as-extruded after etching are included as **Figure 39.4. Figure 39.4a** shows a transverse section with a grain morphology elongated in the extrusion direction, whereas **Figure 39.4b** shows a longitudinal section with apparently equiaxed grains.

AZ31 plate material was also purchased to perform initial rolling trials. This material will also be compared to the microstructure of as-extruded and as-rolled experimental ZK60 material. The initial polishing procedure has been the same as the ZK60, yet AZ31 exhibits much more pitting throughout the process, so the polishing procedure needs to be optimized, along with the etchant.

### 39.3.2 Experimental Material and Heat Treatments

The experimental material is nominally a ZK60 composition, with the substitution of various percentages of Ce for Zr. The compositions of this experimental material are included as **Table 39.1**. The material is varied into three different categories: Low solute (~1% Zn), medium solute (~2.5% Zn), and high solute, (~4% Zn). For each of these categories, there is material that is either complete solid solution, ~1% pinning phases, or ~3% pinning phases. These categories of nominally ZK60 composition allow variation of both total solute and precipitation phase percentages.

Initially proposed heat treatments of these ZK60 experimental materials include both times and temperatures ranging from 300°C-400°C and 6 hours-48 hours. These static recrystallization study heat treatments are included as **Table 39.2** and will be performed after cold rolling. EBSD will be completed after each of the time-temperature combinations in order to calculate percent recrystallization. As results are determined, subsequent time-temperature combinations will be optimized in order to ensure a static recrystallization model is completed with enough temperature and time intervals.

### 39.3.3 Cold Rolling Trials

Pre-straining is necessary to understand the effects of deformation on recrystallization kinetics. Cold rolling is a consistent method for pre-straining and approximately 20-30% deformation is needed for effectiveness [39.11]. Cold rolling will increase hardness uniformly due to an increase in stored strain energy. The grain size should decrease after recrystallization of these cold rolled samples because grain growth is limited by pinning. Sections of each of the 10 extrudates (5 alloy compositions) were machined to the geometry of about ½" x 7/8" x ¼". The compositions of these alloys are included in **Table 39.1.** Each of these sections were rolled to determine the maximum reduction of thickness possible. The exact geometries of these specimens are included in **Table 39.3,** as well as the percent reductions achieved for each sample. This table also includes the calculated strain per pass leading to the reduction of each sample. The goal of these initial trials was to determine the amount of cold work necessary before heat treating to allow for the maximum recrystallization for each time and temperature combination. It was also important to determine a threshold for maximum strain per pass to ensure repeatable results at achieving necessary reduction in future rolling of samples. These initial rolling trials concluded that it is only realistic to get about 20% reduction in thickness and that above ~2.5% strain per pass there are greater quality issues, including cracking and surface defects.

These rolled samples of experimental ZK60 were then compared to AZ31 thin plate rolled samples that were rolled to rolling reductions of 15% and 18%. These AZ31 samples exhibited lower ductility and edge cracking around 10%. Macroscopic pictures of these samples are included as **Figure 39.5.** The center of the AZ31samples were then mounted and polished and will be analyzed to compare the as-rolled microstructure for various rolling reductions to that of the ZK60 as-rolled microstructure.

### 39.3.4 X-Ray Diffraction (XRD) Preliminary Results

A preliminary XRD scan was completed on billet B10, which has the composition of Mg-6.78% Zn-0.31% Ce (wt.%). The goal of using XRD will be to identify precipitates within the structure. This preliminary scan is included as **Figure 39.6**. This scan shows all peaks over a wide range of angles and requires indexing. Further scans will be completed to look into unique peaks to distinguish between precipitate profiles.

### 39.4 Plans for Next Reporting Period

Upcoming plans include further optimizing a low deformation metallographic preparation procedure for ZK60 samples and performing rolling experiments, heat treatments, Gleeble testing, and microstructural analysis. Additional steps will be taken to in the upcoming months to further this project, including:

- Cold rolling of received experimental material.
- Heat treatment at various temperatures (300, 350, and 400 °C) and times (6 - 48 hours) to determine a static recrystallization kinetics model.
- EBSD imaging of ZK60 heat treated specimens to determine percent recrystallization and overall microstructural evolution.
- Dynamic recrystallization study using the Gleeble thermomechanical simulator.

### 39.5 References

[39.1] ASTM Standard: B91-17, Standard Specification for Magnesium-Alloy Forgings, ASTM International.
[39.2] T. Bhattacharjee, T. Sasaki, B. Suh, Role of Zr in the Microstructure Evolution in Mg-Zn-Zr Based Wrought Alloys, Magnesium Technology, (2015) 1-16.
[39.3] J. Cho, S. B. Kang, Deformation and Recrystallization Behaviors in Magnesium Alloys, InTech-Open Science, (2013) 1-4.
[39.4] E. I. Poliak, J.J.Jonas, Initiation of Dynamic Recrystallization in Constant Strain Rate Hot Deformation, ISIJ International. 43 (2003) 684-691.
[39.5] J. Humphreys, G. Rohrer, A. Rollett. Recrystallization and Related Annealing Phenomena, Elsevier, (2013) 494-502.
[39.6] Kaibyshev, R. O., Sitdikov, O. S., Introduction to the Physical Metallurgy of Welding, Physical Metallurgy. 1992, 73-420.
[39.7] Gottstein, G., Kocks, U.F., Thermo-Mechanical Processing of Metallic Materials, Material Science Technology. 1991, 7-158.
[39.8] A.Galiyev, R. Kaibysev, G. Gottstei, Correlation of Plastic Deformation and Dynamic Recrystallization in Magnesium Alloy ZK60, Acta Materialia. 49 (2001) 1199-1207.
[37.9] ASTM Standard: B107/B107M-13, Standard Specification for Magnesium-Alloy Extruded Bars, Rods, Profiles, Tubes, and Wires, ASTM International.
[39.10] Ion, S.E., Humphreys, F.J. and White, S.H., The Effect of Equal Channel Angular Pressing Process on The Microstructure of AZ31 Mg Alloy Strip Shaped Specimens, Acta Materialia. 1982, 145-149.
[39.11] Y. Yuan, A. Ma, J. Jiang, High Mechanical Properties of Rolled ZK60 Mg Alloy through Pre-Equal Channel Angular Pressing, Mechanika. (2016) 256-259.

## 39.6 Figures and Tables

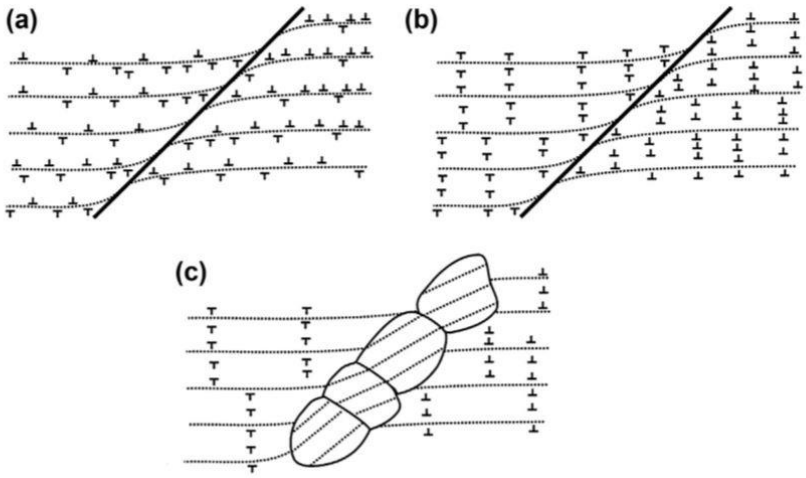


Figure 39.1: Schematic diagram showing proposed mechanism of DRX by progressive lattice rotation and dynamic recovery at grain boundaries in magnesium alloys. (a), (b), and (c) show the progression through initial shear band formation, dynamic recovery of geometrically necessary dislocations, and subgrain/grain formation [39.5].

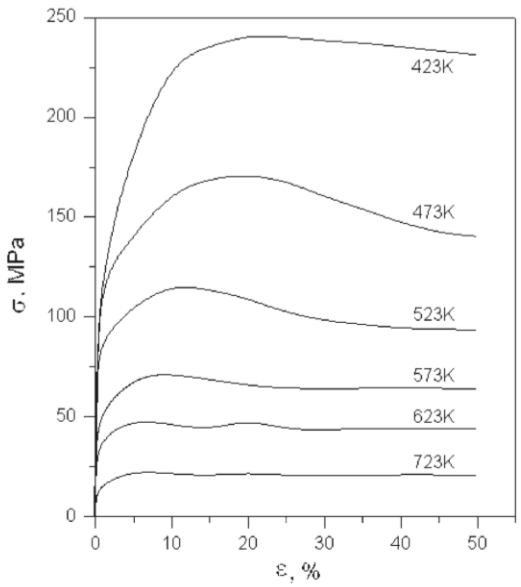


Figure 39.2: Flow curves at various temperatures for ZK60 at constant strain rate (2.8 x $10^{-3}s^{-1}$) uniaxial compression tests [39.8].

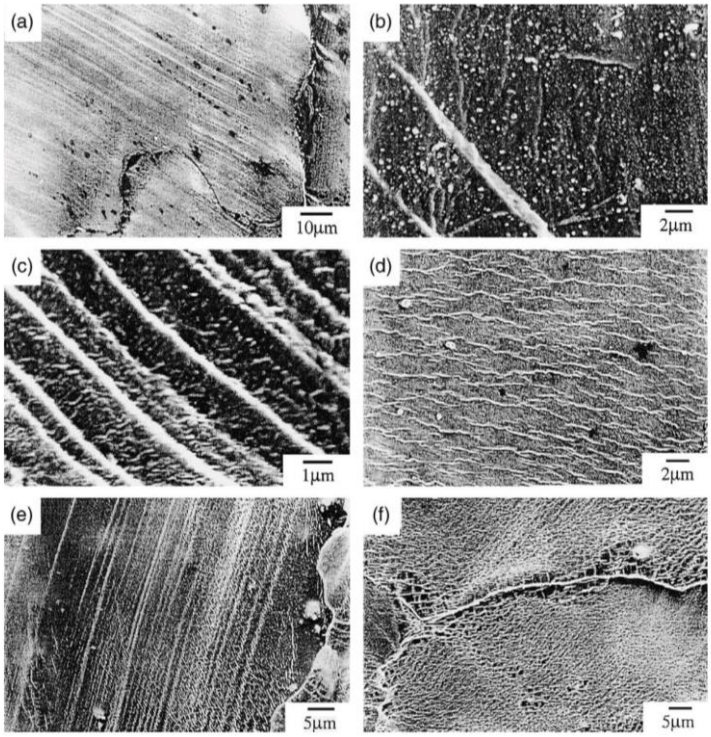


Figure 39.3: SEM secondary electron micrographs of ZK60 post-compression testing. (a) T=423 K, long straight lines of basal slip; (b) T=423 K, short thin lines of $\{11\bar{2}2\}<\bar{1}\bar{1}23>$ slip; (c) T=523 K, lines of basal slip and non-basal slip within body of original grains; (d) T=523K, short wavy lines of a dislocation cross-slip; (e), (f) T=623K, extensive multiple slip [39.8].

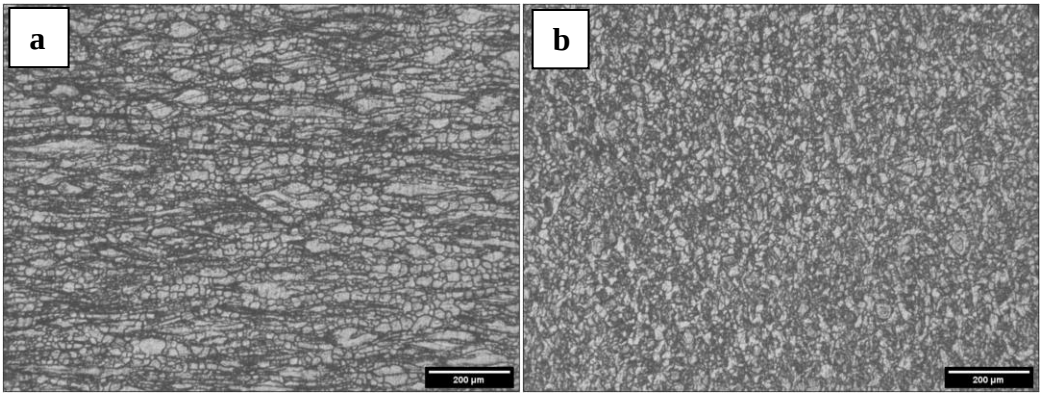


Figure 39.4: Optical micrographs of as-extruded trial ZK60 material (50x): [a] longitudinal to the extrusion direction and [b] transverse to the extrusion direction. These samples were etched with: 3g picric acid, 10mL acetic acid, 70mL ethanol, and 10mL of distilled water.

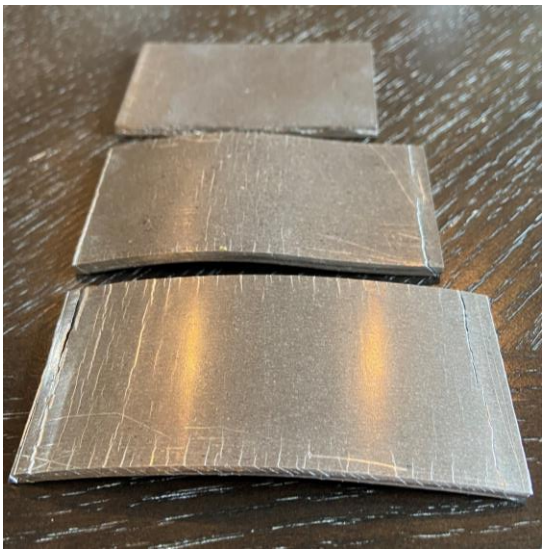

Figure 39.5: Rolled AZ31. From top to bottom: 0% reduction in thickness (not rolled), 15% reduction in thickness, and 18% reduction in thickness. Initial geometry of these samples before rolling is 3” x 1.5” x 0.125”.

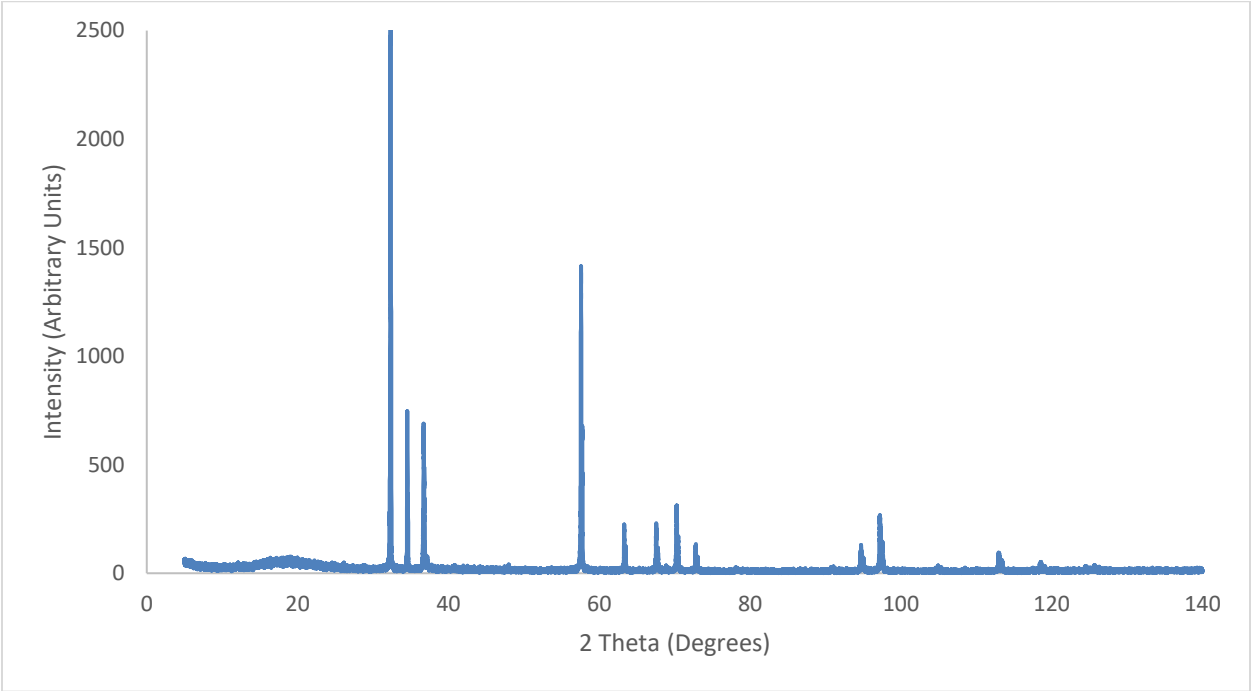


Figure 39.6: XRD scan showing a wide range of 2-Theta angles and peaks of on the experimental ZK60 material of composition: Mg-6.78Zn-0.31Ce (High solute/~ 3% pinning phases).

Table 39.1: Experimental material compositions based on ZK60 alloys (wt.%).

| | **Complete Solid Solution** | **~ 1% pinning phases** | **~ 3% pinning phases** |
|---|---|---|---|
| **Low solute (~ 1%Zn)** | - | Mg-1.40Zn-0.38Ce | - |
| **Med solute (~ 2.5%Zn)** | - | Mg-3.52Zn-0.38Ce | - |
| **High solute (~ 4%Zn)** | Mg-4.21Zn | Mg-5.26Zn-0.12Ce | Mg-6.78Zn-0.31Ce |

Table 39.2: Heat treatment matrix for experimental samples of nominal ZK60 composition. HT=heat treat, Q=quench.

| - | **6 hours** | **8 hours** | **12 hours** | **24 hours** | **48 hours** |
|---|---|---|---|---|---|
| **300 °C/573K** | HT+Q | HT+Q | HT+Q | HT+Q | HT+Q |
| **350 °C/623K** | HT+Q | HT+Q | HT+Q | HT+Q | HT+Q |
| **400 °C/673K** | HT+Q | HT+Q | HT+Q | HT+Q | HT+Q |

Table 39.3: Current rolling trial progress. The rolling procedure was changed for B1-B4 where the first 4 passes were at 0.01” reduction and the remaining were at 0.005” reduction. B5-B10 each pass was set at 0.01” reduction.

| Billet ID | Initial thickness (in) | Final thickness (in) | Passes | Reduction (%) | Strain per pass |
|---|---|---|---|---|---|
| Low solute/ ~ 1% pinning phases | 0.338 | 0.296 | 11 | 12% | N/A |
| Low solute/ ~ 1% pinning phases | 0.321 | 0.281 | 11 | 12% | N/A |
| Med solute/ ~ 1% pinning phases | 0.324 | 0.275 | 12 | 15% | N/A |
| Med solute/ ~ 1% pinning phases | 0.351 | 0.316 | 8 | 10% | 1.25% |
| High solute/ Complete solid solution | 0.365 | 0.275 | 8 | 25% | 3.08% |
| High solute/ Complete solid solution | 0.348 | 0.274 | 9 | 21% | 2.36% |
| High solute/ ~ 1% pinning phases | 0.286 | 0.233 | 8 | 19% | 2.32% |
| High solute/ ~ 1% pinning phases | 0.347 | 0.291 | 9 | 16% | 1.79% |
| High solute/ ~ 3% pinning phases | 0.251 | 0.201 | 8 | 20% | 2.49% |
| High solute/ ~ 3% pinning phases | 0.249 | 0.205 | 8 | 18% | 2.21% |